

# Enhancing Heat Transfer Efficiency in Radiators and Heat Exchanger Through CFD Analysis and Nanofluid Implementation

<sup>1</sup>Amit Kumar, <sup>2</sup>Shamir Daniel, <sup>3</sup>Jeetendra Mishra

<sup>1</sup>M. E Scholar, Department of Mechanical Engineering, Truba Institute of Engineering & Information Technology, Bhopal, MP, India.

<sup>2</sup>Assistant Professor, Department of Mechanical Engineering, Truba Institute of Engineering & Information Technology, Bhopal, MP, India.

<sup>3</sup>Assistant Professor, Department of Mechanical Engineering, Truba Institute of Engineering & Information Technology, Bhopal, MP, India.

Email [amitmechanical27@gmail.com](mailto:amitmechanical27@gmail.com), [shamirdaniel3004@gmail.com](mailto:shamirdaniel3004@gmail.com), [jeetendra.mishra@trubainstitute.ac.in](mailto:jeetendra.mishra@trubainstitute.ac.in)

\* Corresponding Author: Amit Kumar

**Abstract:** *The radiators include heat exchangers that transfer heat from a single material to another for cooling and heating purposes. To examine the thermal performance of the radiator at various heat transfer fluid flow rates while using different coolants, such as deionized water, a blend of ethylene glycol and water (60:40) mixed with Al<sub>2</sub>O<sub>3</sub> nanofluids, a combination of ethylene glycol and water (50:50) mixed with ZnO Nanofluids, and a combination of ethylene glycol and water (60:40) mixed with graphene Oxide, computational and computational fluid dynamic analysis has been To do this, a three-dimensional CAD radiator model was made using the design module of the ANSYS workbench, and a steady state pressure-based absolute velocity version analysis was defined, using the Energy equation for thermal analysis and the K-epsilon RNG viscous simulation using a standard wall function for turbulent flow. Heat transfer fluid mass flow inlets with a range of 180 LPH, 240 PH, 300 LPH, 360 LPH, and 420 LPH have been employed. The heat transfer coefficient increases by 7.9 times at 180 LPH, the Nusselt number increases by 1.77 times at 180 LPH, and the temperature difference increases by 1.67 times at 300 LPH when using a ZnO Nanofluids mixture of ethylene glycol & water (50:50) as opposed to deionized water, according to the results.*

**Keywords:** Radiators, heat exchangers, CFD analysis, nanofluid,

## I. INTRODUCTION

Radiators and exchangers for heat, among other industrial uses, depend on efficient heat transmission since it has a direct influence on how well they work and how much energy they use. The overall efficacy of these systems has been improved by extensive research and development towards improving heat transfer efficiency. The use of nanofluids and computational fluid dynamics (CFD) analyses have both been identified as possible methods for achieving this objective. Many different industries, including the automotive, aerospace, energy production, and electronics sectors, rely heavily on radiators and heat exchangers. Their major job is to move energy from a single medium to another, keeping everything at the right temperature and avoiding overheating. However, because to restrictions regarding the flow of fluid trends, thermal efficiency, and heat transfer coefficients[1], traditional designs frequently struggle to achieve high heat transfer rates.

The design and optimisation of heat transfer systems have undergone a revolution thanks to computational fluid dynamics (CFD) analysis. CFD helps engineers and researchers to comprehend and visualise the complicated fluids circulation and transfer of heat processes inside radiators and heat exchangers by using computerised simulations and mathematical modelling approaches. By identifying potential areas for improvement and examining cutting-edge designs, this knowledge helps to increase heat transfer efficiency. The use of nanofluids has drawn a lot of interest recently as a potential way to improve heat transfer effectiveness. Nanoparticle suspensions in base fluids are known as nanofluids. These nanoparticles can be metallic or non-metallic. Increased thermal conductivity and enhanced surface area, two distinctive characteristics of nanoparticles, can considerably improve the base fluid's capacity for heat transmission. These nanoparticles change the working fluid's thermophysical characteristics, enhancing convection heat transfer and lowering thermal resistance.

Radiators and exchangers for heat, among other industrial uses, depend on efficient heat transmission since it has a direct influence on how well they work and how much energy they use. The overall efficacy of these systems has been improved by extensive research and development towards improving heat transfer efficiency. The use of nanofluids and computational fluid dynamics (CFD) analyses have both been identified as possible methods for achieving this objective. Many different industries, including the automotive, aerospace, energy production, and electronics sectors, rely heavily on radiators and heat exchangers. Their major job is to move energy from a single medium to another, keeping everything at the right temperature and avoiding overheating. However, because to restrictions regarding the flow of fluid trends, thermal efficiency, and heat transfer coefficients[1], traditional designs frequently struggle to achieve high heat transfer rates.

The design and optimisation of heat transfer systems have undergone a revolution thanks to computational fluid dynamics (CFD) analysis. CFD helps engineers and researchers to comprehend and visualise the complicated fluids circulation and transfer of heat processes inside radiators and heat exchangers by using computerised simulations and mathematical modelling approaches. By identifying potential areas for improvement and examining cutting-edge designs, this knowledge helps to increase heat transfer efficiency. The use of nanofluids has drawn a lot of interest recently as a potential way to improve heat transfer effectiveness. Nanoparticle suspensions in base fluids are known as nanofluids. These nanoparticles can be metallic or non-metallic. Increased thermal conductivity and enhanced surface area, two distinctive characteristics of nanoparticles, can considerably improve the base fluid's capacity for heat transmission. These nanoparticles change the working fluid's thermophysical characteristics, enhancing convection heat transfer and lowering thermal resistance.

## II. LITERATURE REVIEW

**R. Prasanna Shankara et al. (2022) [2]** Recent studies showed that nanofluids are considered as a promising way to enhance the heat transfer properties of coolants. Currently, in a car radiator forced convection heat transfer method is carried out to cool circulating fluid. The mixture of water with either ethylene or propylene-glycol is necessary to lower its freezing point and eliminate ice formation. The maximum Nusselt number value of 192 at 420 LPH was observed for 60:40 EG/DW-based GO nanofluid as compared with 20:80, 30:70 EG/DW-based GO nanofluid. It is estimated that by replacing conventional coolant with this nanofluid, reduction in the frontal area of radiator is done which gives more flexibility for industrial design, more eco-friendly vehicle which produces less drag and hence less the fuel cost.

**Pan, A.-X. et al. (2021) [3]** The radiator is a sandwich structure with many fins brazed on the clapboards to dissipate the heat generated from the transformers, so it is an important device for ensuring safe operation of the transformers. However, many radiators failed only after one and a half years of service although their design life is five years. The analysis results showed that the microscopic holes resulting in the leakages in the clapboard and brazed joint were caused by pitting corrosion along the air side of the clapboard. The inappropriate design of the fin structure and the unqualified brazing process were identified to be the two root causes leading to the pitting corrosion on the clapboard of the radiators. Countermeasures were thus put forward to solve the corresponding problems.

**Ijaz, H. Et al. (2020) [4]** This study includes the simulation based investigation of thermal characteristics of graphene doped nano coolant in car radiator. A small radiator part is considered for the system analysis, which is modeled using Solid-works software package. CFD analysis is carried out using ANSYS Fluent module. Typically, 9.68 K, 10.89 K and 11.9 K temperature drop is observed for 6%, 8% and 10% of GO nano particles, respectively. With the percentage increase in the addition of nano particles, the effectiveness of the radiator also increases. Maximum increase in percentage effectiveness of 97.49% is at 10% volume fraction of GO nanoparticles in water. Using this type of coolant for heat transfer enhancement can help in developing more compact and lightweight radiators for cars and can be applied in other industries as well.

**Abhilash, P. et al. (2021) [5]** Automobile radiators are important for the performance enhancement and heat dissipation. Flow behaviour is the important factor in designing the radiator. In this study aluminium oxide nanofluid have been considered with increasing rate of heat transfer with different mass flow rate in fixed and helical pipe radiator using Computational fluid dynamics (CFD) to study the flow of fluid. The purpose of study to propose the suitable model for enhancement of heat transfer at specific coolant. Computational fluid dynamic diagnosis was diagnosed on pursuance of quite fluids with thermal evaluation was completed by Analytical systems. Three dimensional model was finished using Creo parametric tool. Aluminum oxide blend with water at mixed proportion ration for better heat transfer rate in radiator.

**Kirubagharan, R. et al. (2020) [6]** Impacts of the glow move execution of a framework or motor are frequently improved utilizing a blend of the numerous inactive techniques, to be specific nano liquid and different sorts of cylinder geometric and material of cylinder during this paper The impact of cylinder geometry towards the glow move execution assessed. The constrained convective warmth move Performance, erosion factor and divider shear pressure are considered utilizing various geometries. The thermo-physical properties like thickness, heat, consistency and warm conductivity are investigated for the assurance of cylinder geometry. The different cylinder geometries in recreation work are broke down specifically roundabout cylinder, foil tube and rectangular cylinder. In the meantime, the foil tube has more noteworthy warmth move coefficient with contrasted with the roundabout cylinder.

**Nasiri, A. et al. (2019) [7]** Detection of faults and intelligent monitoring of equipment operations are essential for modern industries. Cooling radiator condition is one of the factors that affects engine performance. This paper proposes a novel and accurate radiator condition monitoring and intelligent fault detection based on thermal images and using a deep convolutional neural network (CNN) which has a specific configuration to combine the feature extraction and classification steps. Evaluation of the model demonstrates that leads to results better than traditional computational intelligence methods, such as an artificial neural network, and can be employed with high performance and accuracy for fault diagnosis and condition monitoring of the cooling radiator under various working circumstances.

### III. METHODOLOGY

The radiators are exchangers that transfer heat from a single substance to another for cooling and heating purposes. The radiator constantly serves as a heat source for the area around it, whether it is to heat the area or to cool the water or coolant provided to it, as in the case of cooling an automobile engine. Instead of using thermal radiation, the majority of radiators use convection to transmit heat. Heat radiation, convection into air that is moving or water, and conductivity into the air or liquid are the three ways that heat is transferred from a radiator. Multiple fins interacting with the tube holding the liquid pushed through the radiator will enhance the surface area accessible for the exchange of heat with the surroundings. Air that comes into touch with the fins radiates heat.

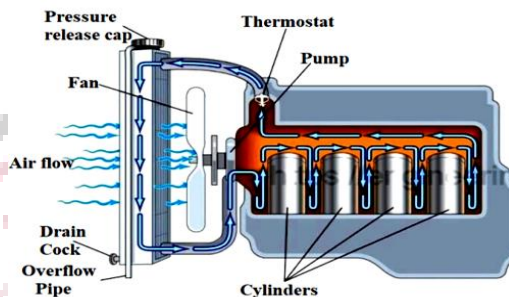


**Figure 1** Concept of heat transfer of engine through radiator

Investigation of system involving fluid flow and heat transfer using computer-based simulation is known as computational fluid dynamics. Ansys Fluent is used in the current work's mathematical fluid dynamics analysis for the radiator. This computational study is carried out using the governing equations, including the continuity equation, species transfer, velocity equation, and energy equation.

After the radiator's three-dimensional CAD geometry is created, it is transferred for meshing. Mesh is a crucial operation in which the radiator's CAD geometry is separated into numerous nodes and elements. The process of breaking down the geometry into little parts is known as meshing. The total number of nodes and elements in the current work is 1238405 and 808251, respectively. Tetrahedral and hexahedral elements are utilised due to the radiator's complicated design, which is seen in figure 4.4. For meshing, a minimal component thickness of 0.5 mm and a 1.2 growth rate have been used.

By varying the flow rate of the heat transfer fluid from 180 LPH to 420 LPH, it was possible to examine the heat transfer capacity of the radiator through graphene Oxide/ethylene glycol:water (60:40) and Deionized water as a coolant. It was found that the maximum improvement in the rate of heat transfer of graphene Oxide/ethylene glycol:water (60:40) coolant compared to with Deionized water was 83.3% with 0.8% error. The comparison of the aforementioned results reveals excellent agreement between the base study and the current work; hence, it is necessary to conduct additional heat transfer analysis using various coolants while adding nanofluids and maintaining the same boundary conditions.

### IV. RESULT AND DISCUSSION

The main objective of the present work to investigate the heat transfer performance of the radiator at different flow rate of the heat transfer fluid by using various coolants such as deionized water, mixture of ethylene glycol and water (60:40) mixed with Al<sub>2</sub>O<sub>3</sub> nanofluid, mixture of ethylene glycol and water (50:50) mixed with ZnO nanofluid, and mixture of ethylene glycol and water (60:40) mixed with graphene oxide (GO) nanofluid. For that three dimensional CAD model of radiator has been created in design modular of ANSYS workbench and perform CFD analysis by defining the Steady state pressure based absolute velocity formulation analysis where Energy equation is used for thermal analysis, K-epsilon RNG viscous model with standard wall function has been used for turbulent flow. Mass flow inlet of heat transfer fluid ranging from 180 LPH, 240 PH, 300 LPH, 360 LPH and 420 LPH has been used. SIMPLE scheme for the pressure-velocity coupling has been define for solution method and second order upwind for the Momentum and Energy equation have been applied for this analysis. Various results of heat transfer rate, heat transfer coefficient, temperature difference and Nusselt numbers obtained in the form of contour diagram table and graphs have been discussed in this chapter.

#### A. Computational Fluid Dynamics Analysis for Radiator using Deionized Water Ranging from 180-420 LPH

- Computational Fluid Dynamics Analysis for Radiator using Deionized Water at 180 LPH

After performing Computational fluid dynamic analysis on radiator using deionized water at 180 LPH with inlet temperature of 90°C for the temperature distribution, the outlet temperature of 74.28°C with the temperature difference of 15.72 degree has been observed

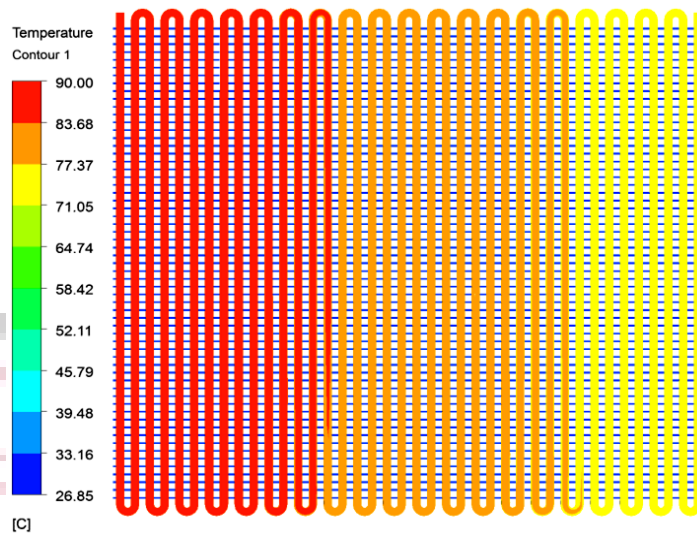


Figure 2 Temperature distribution using deionized water at 180LPH

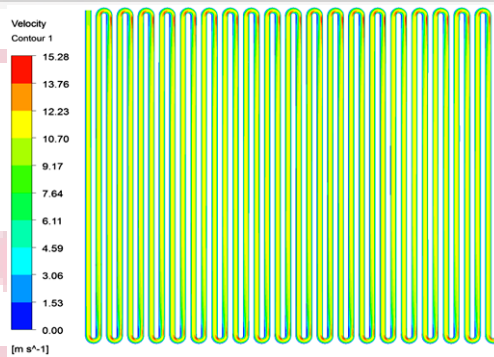


Figure 3 Velocity distribution using deionized water at 180LPH

- Computational fluid dynamics analysis for radiator using deionized water at 240 LPH

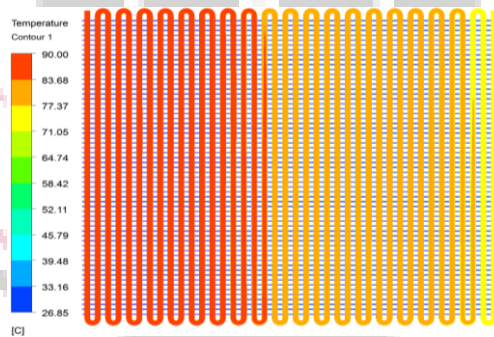


Figure 4 Temperature distribution using deionized water at 240LPH

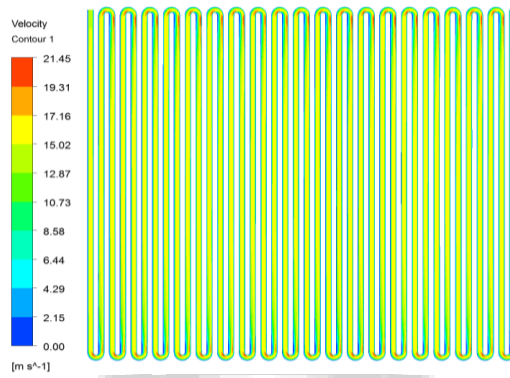


Figure 5 Velocity distribution using deionized water at 240LPH

- Computational fluid dynamics analysis for radiator using deionized water at 300 LPH

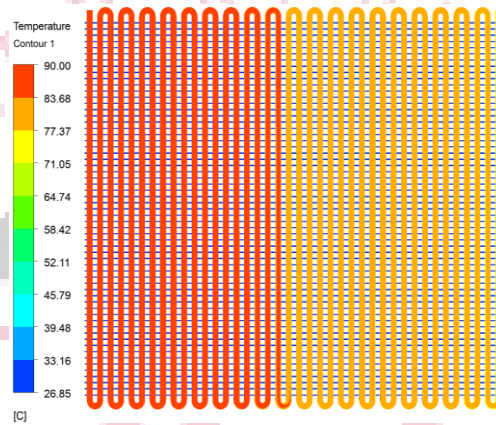


Figure 6 Temperature distribution using deionized water at 300LPH

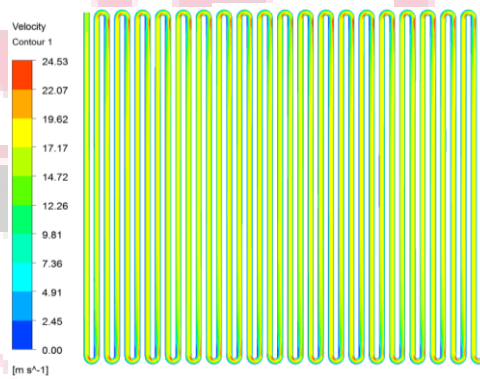


Figure 7 Velocity distribution using deionized water at 300LPH

- Computational fluid dynamics analysis for radiator using deionized water at 360 LPH

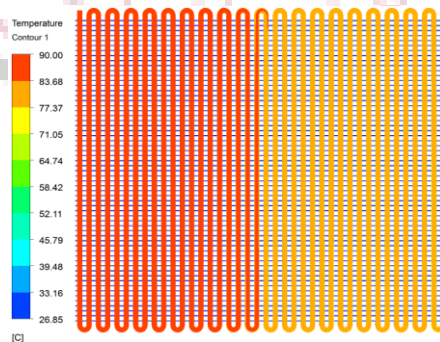


Figure 8 Temperature distribution using deionized water at 360LPH

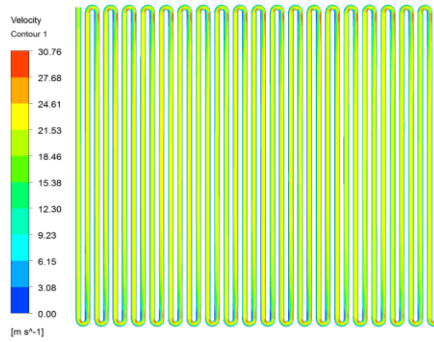


Figure 9 Velocity distribution using deionized water at 360LPH

- Computational fluid dynamics analysis for radiator using deionized water at 420 LPH

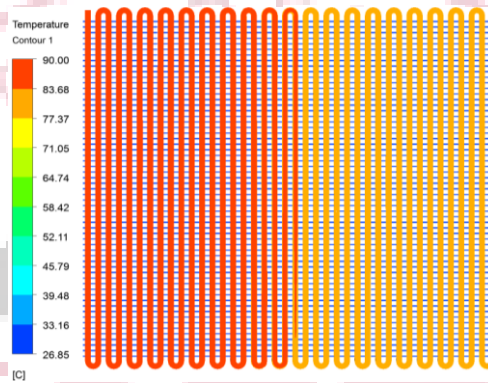


Figure 10 Temperature distribution using deionized water at 420LPH

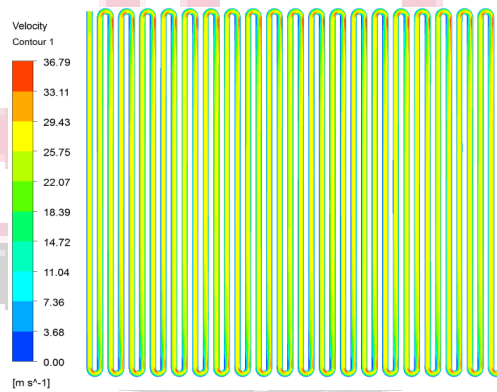


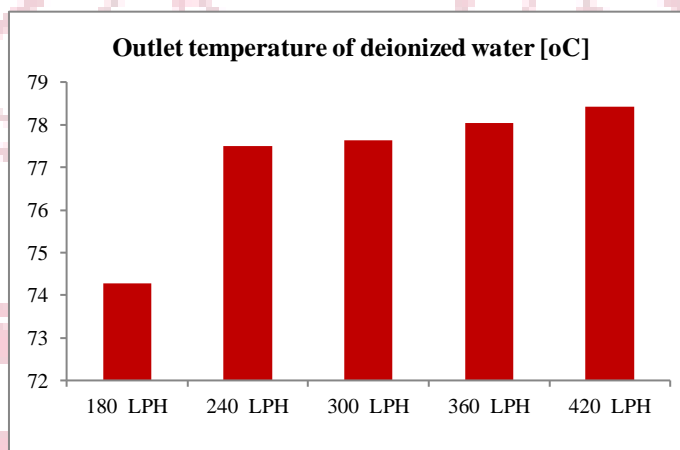
Figure 11 Velocity distribution using deionized water at 420LPH

Table 1 Comparative results of temperature difference & heat transfer rate for Deionized water

Mass flow rate [LPH]	Inlet Temperature [°C]	Outlet temp [°C]	Temperature Difference $\Delta T$	Heat transfer rate [W]
180	90	74.28	15.72	3806.25
240	90	77.49	12.51	4240.63
300	90	77.63	12.37	4792.20
360	90	78.05	11.95	5786.86
420	90	78.42	11.58	6729.22

**Table 2 Comparative results of Reynolds number, Nusselt number & heat transfer coefficient for Deionized water**

Mass flow rate [LPH]	Reynolds number [Re]	Nusselt number [Nu]	Convective heat transfer coefficient [W/m <sup>2</sup> K]
180	5245.166	42.58	3122.58
240	8614.17	60.97	4470.97
300	12275.58	76.45	5606.45
360	15752.09	86.13	6316.13
420	18089.02	98.71	7238.71



**Figure 12 Outlet temperature of deionized water**

From the above graph it has been observed that as the flow rates of the coolant were increased the outlet temperature increases, at 180 LPH 74.28 °C, at 240 LPH 77.49 °C, at 300 LPH 77.63 °C, at 360 LPH 78.05 °C & at 420 LPH 78.42 °C. The maximum outlet temperature of 5.578 % increased at 420 LPH as compared with 180 LPH.

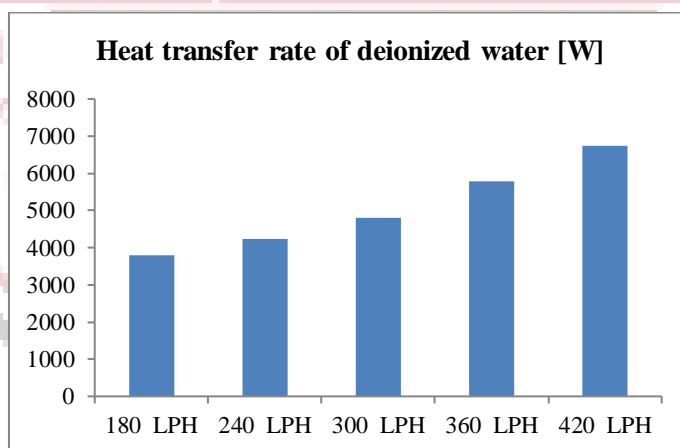


**Figure 13 Heat transfer rate of deionized water**

From the above graph it has been observed that as the flow rates of the coolant were increased the heat transfer rate increases, at 180 LPH 3806.25 W, at 240 LPH 4240.63 W, at 300 LPH 4792.2 W, at 360 LPH 5786.86 W & at 420 LPH 6792.22 W. The maximum heat transfer rate of 76.79 % increased at 420 LPH as compared with 180 LPH.

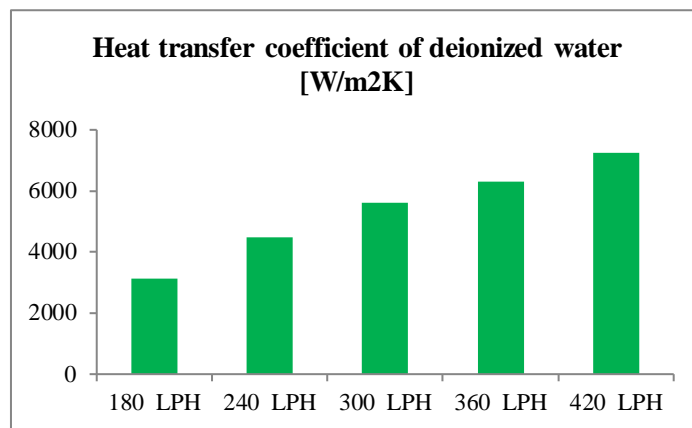


**Figure 14 Heat transfer coefficient of deionized water**

From the above graph it has been observed that as the flow rates of the coolant were increased the heat transfer coefficient increases, at 180 LPH 3122.58 W/m<sup>2</sup>K, at 240 LPH 4470.97W/m<sup>2</sup>K, at 300 LPH 5606.45W/m<sup>2</sup>K, at 360 LPH 6316.13W/m<sup>2</sup>K & at 420 LPH 7238.71W/m<sup>2</sup>K. The maximum heat transfer rate of 1.32 times increased at 420 LPH as compared with 180 LPH.

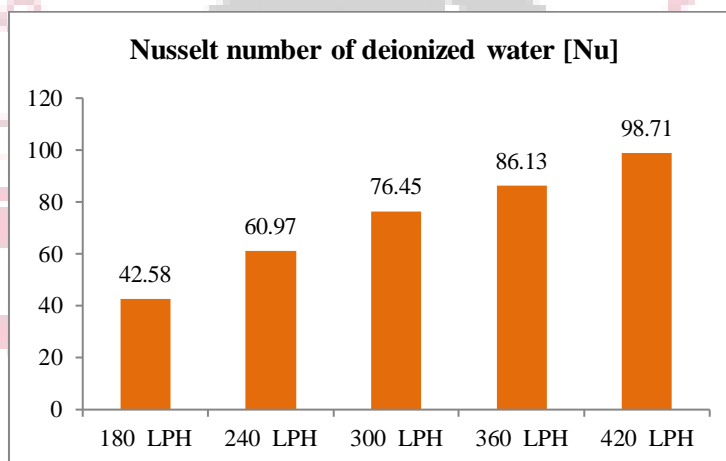


**Figure 15 Nusselt number of deionized water**

From the above graph it has been observed that as the flow rates of the coolant were increased the value of Nusselt number increases, at 180 LPH 42.58, at 240 LPH 60.97, at 300 LPH 76.45, at 360 LPH 86.13 & at 420 LPH 98.71. The maximum Nusselt number of 1.32 times increased at 420 LPH as compared with 180 LPH.

## **B. Computational Fluid Dynamics Analysis for Radiator using Al<sub>2</sub>O<sub>3</sub> Nanofluid Mixture of Ethylene Glycol and Water Ranging from 180-420 LPH**

### **• Computational Fluid Dynamics Analysis for Radiator using Al<sub>2</sub>O<sub>3</sub> Nanofluid Mixture of Ethylene Glycol and Water (60:40) at 180 LPH**

After performing Computational fluid dynamic analysis on radiator using Al<sub>2</sub>O<sub>3</sub> nanofluid mixture of ethylene glycol and water (60:40) at 180 LPH with inlet temperature of 90°C for the temperature distribution, the outlet temperature of 61.60°C with the temperature difference of 28.40 degree has been observed.



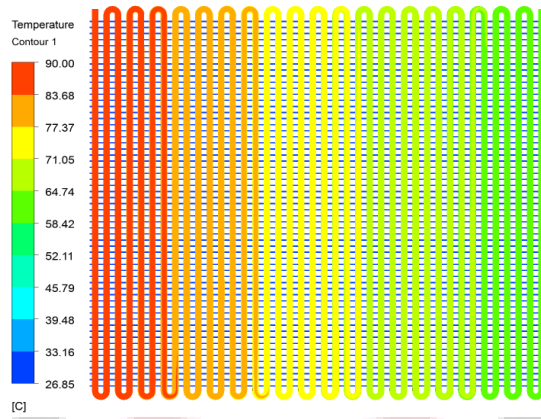


Figure 16 Temperature distribution for Al<sub>2</sub>O<sub>3</sub> nanofluid mixture of ethylene glycol and water (60:40) at 180 LPH

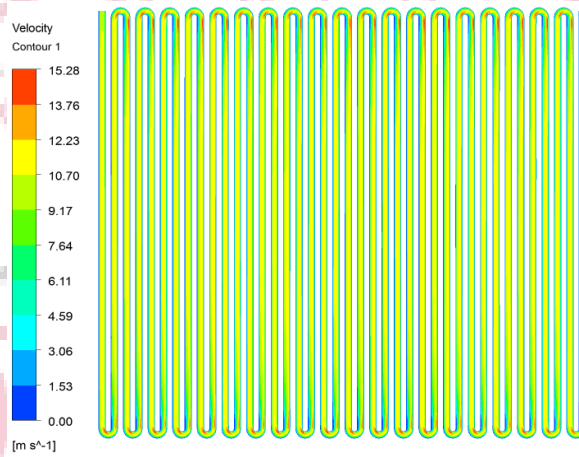


Figure 17 Velocity distribution for Al<sub>2</sub>O<sub>3</sub> nanofluid mixture of ethylene glycol and water (60:40) at 180 LPH

- **Computational Fluid Dynamics Analysis for Radiator using Al<sub>2</sub>O<sub>3</sub> Nanofluid Mixture of Ethylene Glycol and Water (60:40) at 240 LPH**

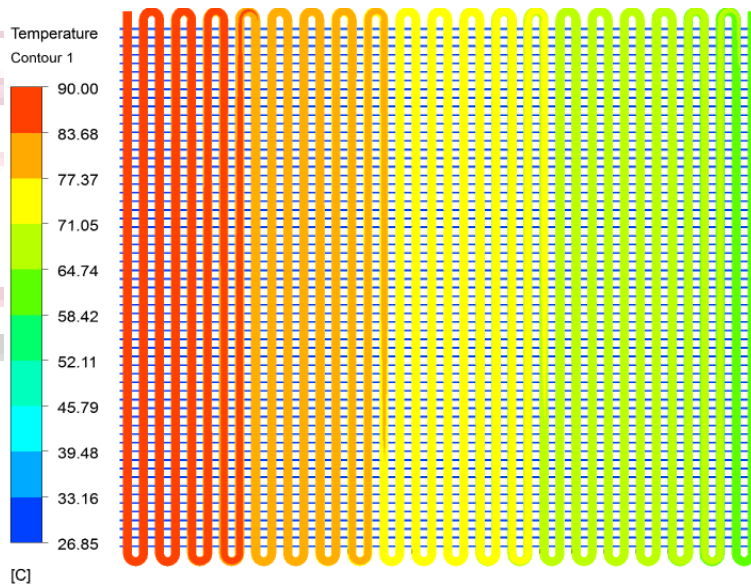


Figure 18 Temperature distribution for Al<sub>2</sub>O<sub>3</sub> nanofluid mixture of ethylene glycol and water (60:40) at 240 LPH

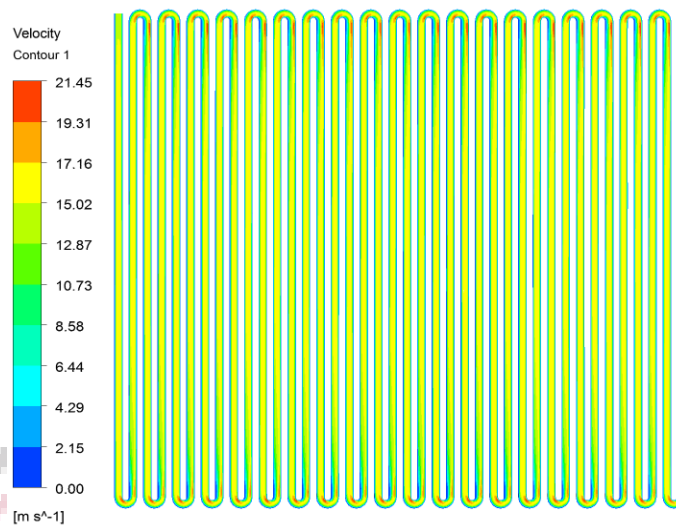


Figure 19 Velocity distribution for Al<sub>2</sub>O<sub>3</sub> nanofluid mixture of ethylene glycol and water (60:40) at 240 LPH

- Computational Fluid Dynamics Analysis for Radiator using Al<sub>2</sub>O<sub>3</sub> Nanofluid Mixture of Ethylene Glycol and Water (60:40) at 300 LPH

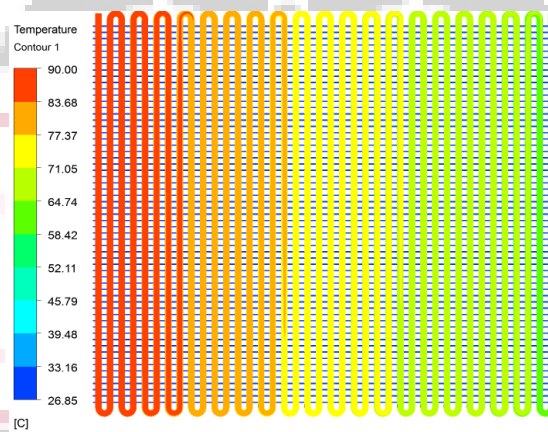


Figure 20 Temperature distribution for Al<sub>2</sub>O<sub>3</sub> nanofluid mixture of ethylene glycol and water (60:40) at 300 LPH

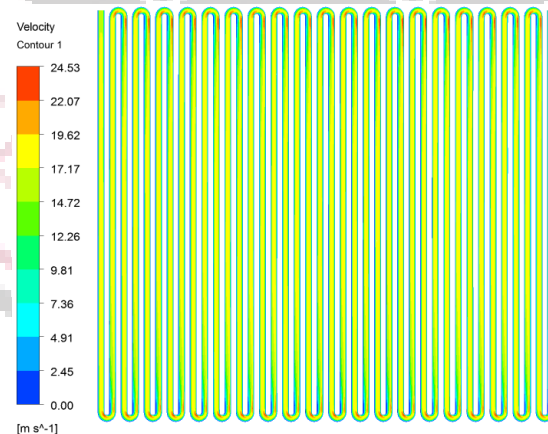


Figure 21 Velocity distribution for Al<sub>2</sub>O<sub>3</sub> nanofluid mixture of ethylene glycol and water (60:40) at 300 LPH

- Computational Fluid Dynamics Analysis for Radiator using Al<sub>2</sub>O<sub>3</sub> Nanofluid Mixture of Ethylene Glycol and Water (60:40) at 360 LPH

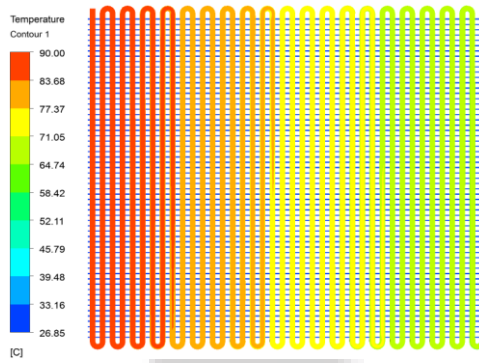


Figure 22 Temperature distribution for Al<sub>2</sub>O<sub>3</sub> nanofluid mixture of ethylene glycol and water (60:40) at 360 LPH

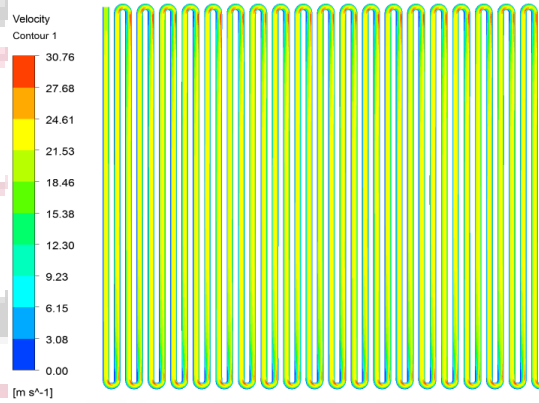


Figure 23 Velocity distribution for Al<sub>2</sub>O<sub>3</sub> nanofluid mixture of ethylene glycol and water (60:40) at 360 LPH

- Computational fluid Dynamics Analysis for Radiator using Al<sub>2</sub>O<sub>3</sub> Nanofluid Mixture of Ethylene Glycol and Water (60:40) at 420 LPH

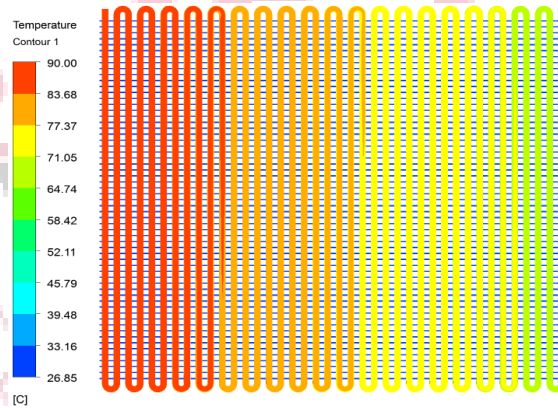


Figure 24 Temperature distribution for Al<sub>2</sub>O<sub>3</sub> nanofluid mixture of ethylene glycol and water (60:40) at 420 LPH

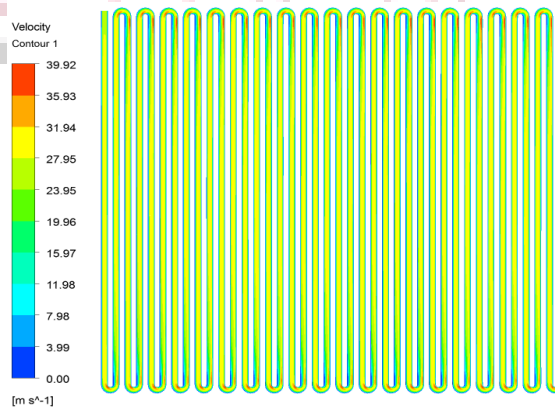


Figure 25 Velocity distribution for Al<sub>2</sub>O<sub>3</sub> nanofluid mixture of ethylene glycol and water (60:40) at 420 LPH

**Table 3 Comparative results of temperature difference & heat transfer rate for Al<sub>2</sub>O<sub>3</sub> nanofluid mixture of ethylene glycol and water (60:40)**

Mass flow rate [LPH]	Inlet Temperature [°C]	Outlet temp [°C]	Temperature Difference ΔT	Heat transfer rate [W]
180	90	61.60	28.40	5007.89
240	90	63.87	26.13	6450.65
300	90	63.89	26.11	7366.53
360	90	67.54	22.46	8713.02
420	90	69.28	20.72	9499.47

**Table 4 Comparative results of Reynolds number, Nusselt number & heat transfer coefficient for Al<sub>2</sub>O<sub>3</sub> nanofluid mixture of ethylene glycol and water (60:40)**

Mass flow rate [LPH]	Reynolds number [Re]	Nusselt number [Nu]	Convective heat transfer coefficient [W/m <sup>2</sup> K]
180	13215.73	99.47	14622.38
240	18502.02	130.20	19139.06
300	21145.16	144.88	21296.79
360	26431.45	173.19	25459.05
420	31717.74	200.39	29456.91

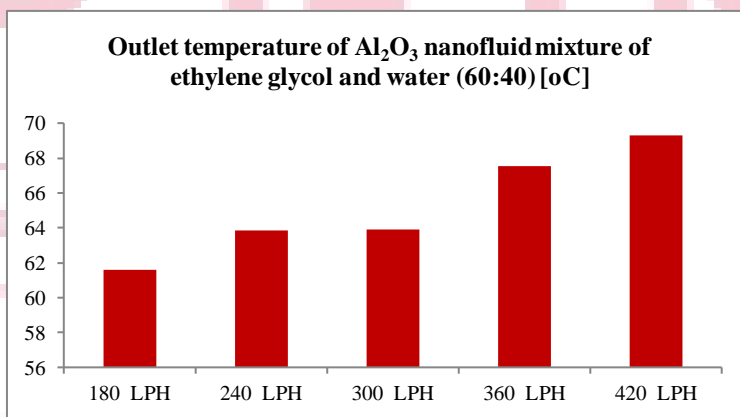


**Figure 26 Outlet temperature of Al<sub>2</sub>O<sub>3</sub> nanofluid mixture of ethylene glycol and water (60:40)**

From the above graph it has been observed that as the flow rates of the nanofluid coolant were increased the outlet temperature increases, at 180 LPH 61.6 °C, at 240 LPH 63.87 °C, at 300 LPH 63.89 °C, at 360 LPH 67.54 °C & at 420 LPH 69.28 °C. The maximum outlet temperature of 12.5 % increased at 420 LPH as compared with 180 LPH.

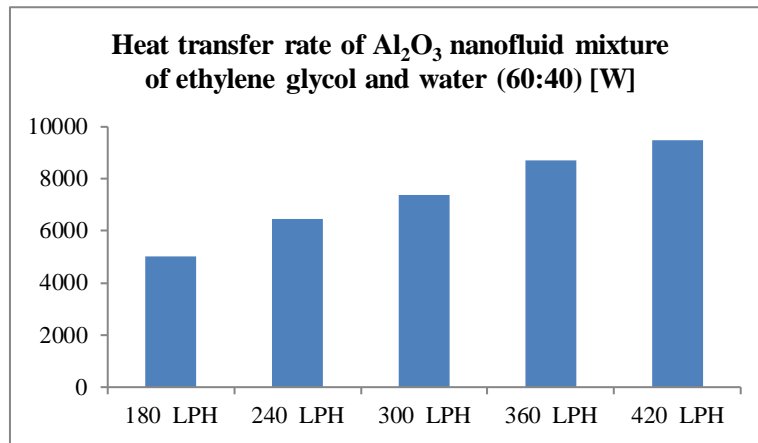


**Figure 27 Heat transfer rate of Al<sub>2</sub>O<sub>3</sub> nanofluid mixture of ethylene glycol and water (60:40)**

From the above graph it has been observed that as the flow rates of the nanofluid coolant were increased the heat transfer rate increases, at 180 LPH 5007.89 W, at 240 LPH 6450.65 W, at 300 LPH 7366.53 W, at 360 LPH 8713.02 W & at 420 LPH 9499.47 W. The maximum heat transfer rate of 89.69 % increased at 420 LPH as compared with 180 LPH.

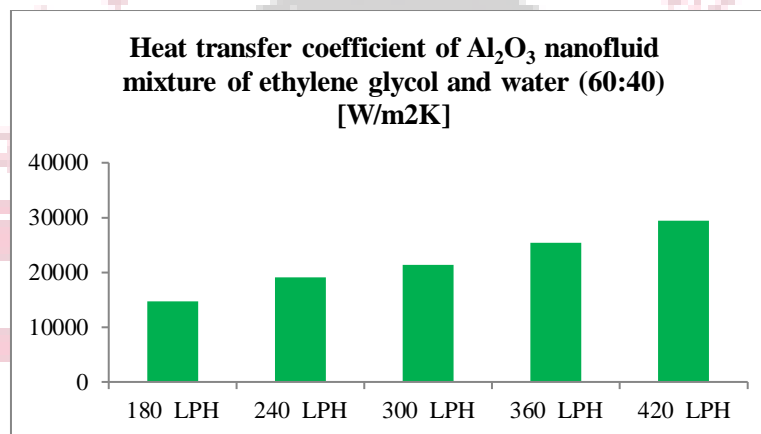


**Figure 28 Heat transfer coefficient of Al<sub>2</sub>O<sub>3</sub> nanofluid mixture of ethylene glycol and water (60:40)**

From the above graph it has been observed that as the flow rates of the nanofluid coolant were increased the heat transfer coefficient increases, at 180 LPH 14622.38 W/m<sup>2</sup>K, at 240 LPH 19139.06 W/m<sup>2</sup>K, at 300 LPH 21296.79 W/m<sup>2</sup>K, at 360 LPH 25459.05 W/m<sup>2</sup>K & at 420 LPH 29456.91 W/m<sup>2</sup>K. The maximum heat transfer rate of 1.015 times increased at 420 LPH as compared with 180 LPH.

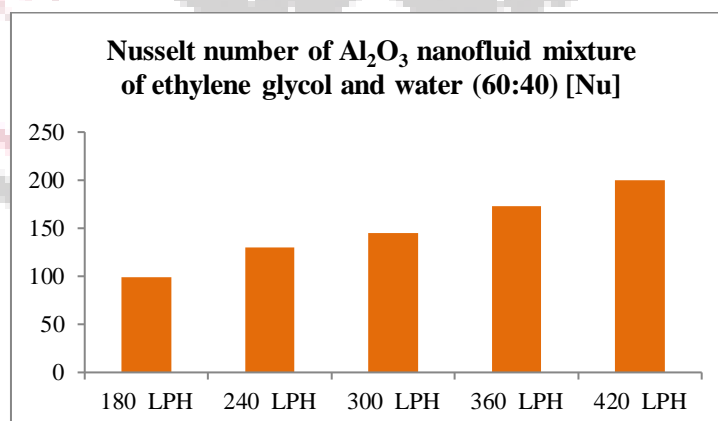


**Figure 29 Nusselt number of Al<sub>2</sub>O<sub>3</sub> nanofluid mixture of ethylene glycol and water (60:40)**

From the above graph it has been observed that as the flow rates of the nanofluid coolant were increased the value of Nusselt number increases, at 180 LPH 99.47, at 240 LPH 130.2, at 300 LPH 144.88, at 360 LPH 173.19 & at 420 LPH 200.39. The maximum Nusselt number of 1.015 times increased at 420 LPH as compared with 180 LPH.

### C. Computational Fluid Dynamics Analysis for Radiator using ZnO Nanofluid Mixture of Ethylene Glycol and Water Ranging from 180-420 LPH

- Computational Fluid Dynamics Analysis for Radiator using ZnO Nanofluid Mixture of Ethylene Glycol and Water (50:50) at 180 LPH

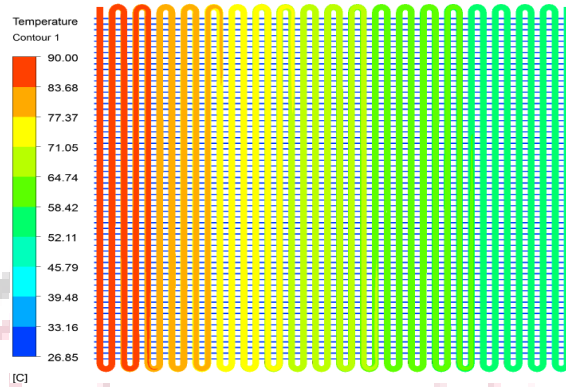


Figure 30 Temperature distribution for ZnO nanofluid mixture of ethylene glycol and water (50:50) at 180 LPH

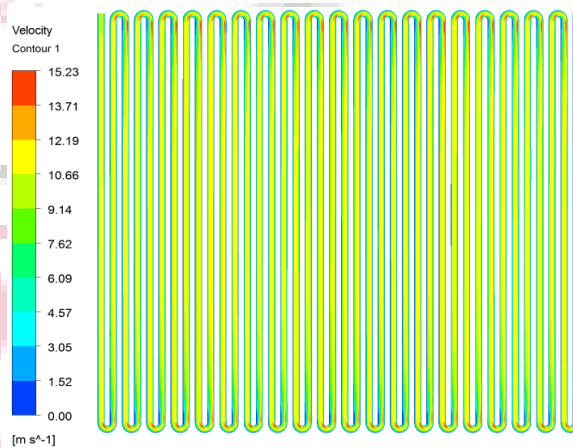


Figure 31 Velocity distribution for ZnO nanofluid mixture of ethylene glycol and water (50:50) at 180 LPH

- Computational Fluid Dynamics Analysis for Radiator using ZnO Nanofluid Mixture of Ethylene Glycol and Water (50:50) at 240 LPH

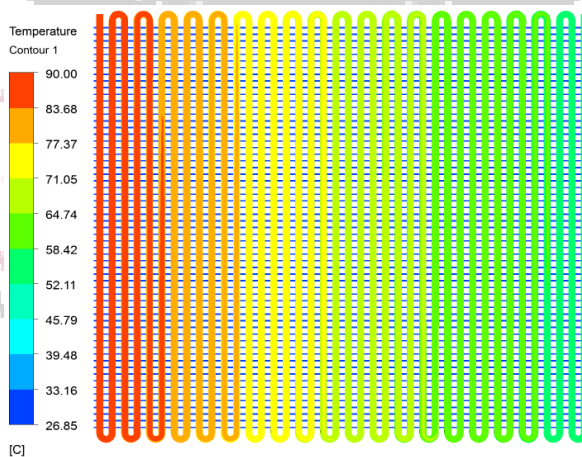


Figure 32 Temperature distribution for ZnO nanofluid mixture of ethylene glycol and water (50:50) at 240 LPH

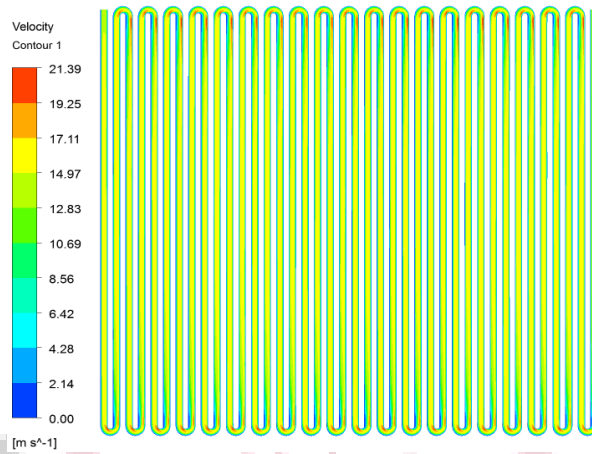


Figure 33 Velocity distribution for ZnO nanofluid mixture of ethylene glycol and water (50:50) at 240 LPH

- Computational Fluid Dynamics Analysis for Radiator using ZnO Nanofluid Mixture of Ethylene Glycol and Water (50:50) at 300 LPH

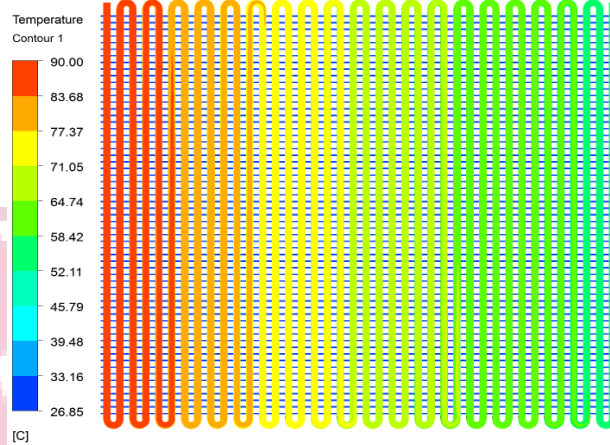


Figure 34 Temperature distribution for ZnO nanofluid mixture of ethylene glycol and water (50:50) at 300 LPH

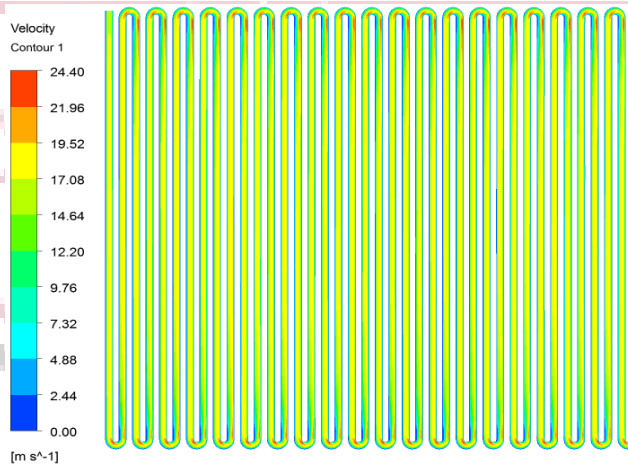
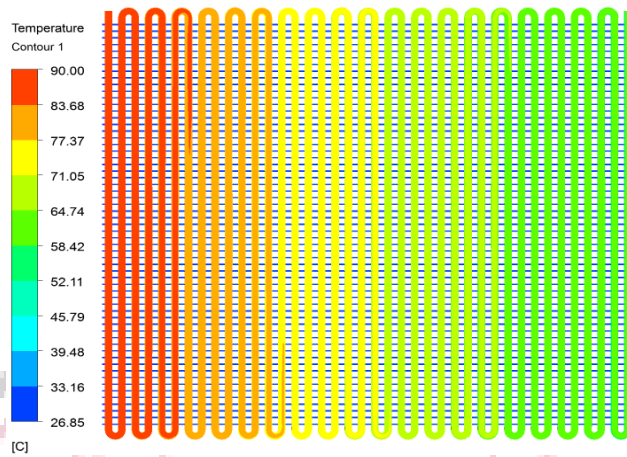
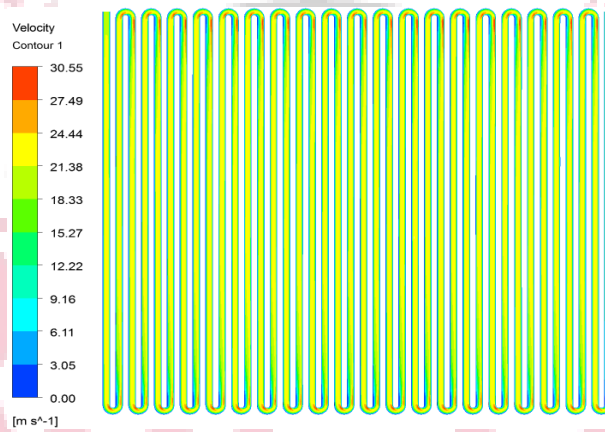


Figure 35 Velocity distribution for ZnO nanofluid mixture of ethylene glycol and water (50:50) at 300 LPH

- **Computational Fluid Dynamics Analysis for Radiator using ZnO Nanofluid Mixture of Ethylene Glycol and Water (50:50) at 360 LPH**



**Figure 36 Temperature distribution for ZnO nanofluid mixture of ethylene glycol and water (50:50) at 360 LPH**



**Figure 37 Velocity distribution for ZnO nanofluid mixture of ethylene glycol and water (50:50) at 360 LPH**

- **Computational Fluid Dynamics Analysis for Radiator using ZnO Nanofluid Mixture of Ethylene Glycol and Water (50:50) at 420 LPH**

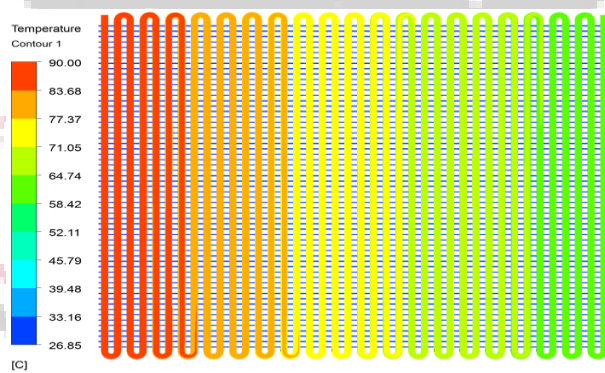


**Figure 38 Temperature distribution for ZnO nanofluid mixture of ethylene glycol and water (50:50) at 420 LPH**



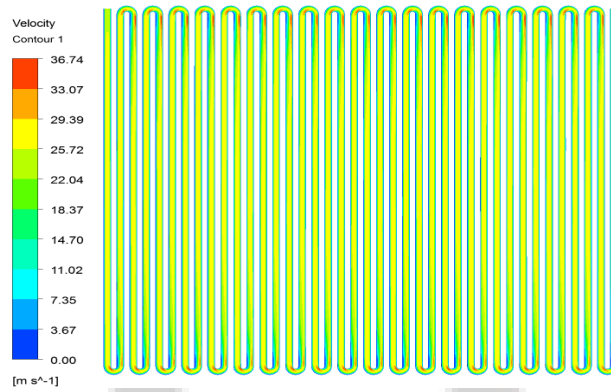


Figure 39 Velocity distribution for ZnO nanofluid mixture of ethylene glycol and water (50:50) at 420 LPH

Table 5 Comparative results of temperature difference & heat transfer rate for EG:W/ ZnO (50:50)

Mass flow rate [LPH]	Inlet Temperature [°C]	Outlet temp [°C]	Temperature Difference $\Delta T$	Heat transfer rate [W]
180	90	53.14	36.86	7402.59
240	90	56.54	33.46	9407.68
300	90	56.86	33.14	10648.81
360	90	59.02	30.98	12443.43
420	90	61.8	28.2	13592.17

Table 6 Comparative results of Reynolds number, Nusselt number & heat transfer coefficient for EG:W/ ZnO (50:50)

Mass flow rate [LPH]	Reynolds number [Re]	Nusselt number [Nu]	Convective heat transfer coefficient [W/m <sup>2</sup> K]
180	23709.68	118.25	27908.43
240	33193.56	154.78	36529.00
300	37935.49	172.23	40647.27
360	47419.37	205.89	48591.40
420	56903.24	238.22	56221.75

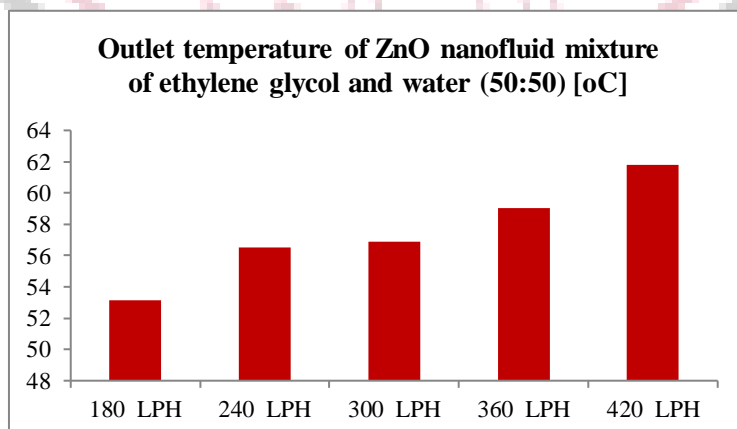
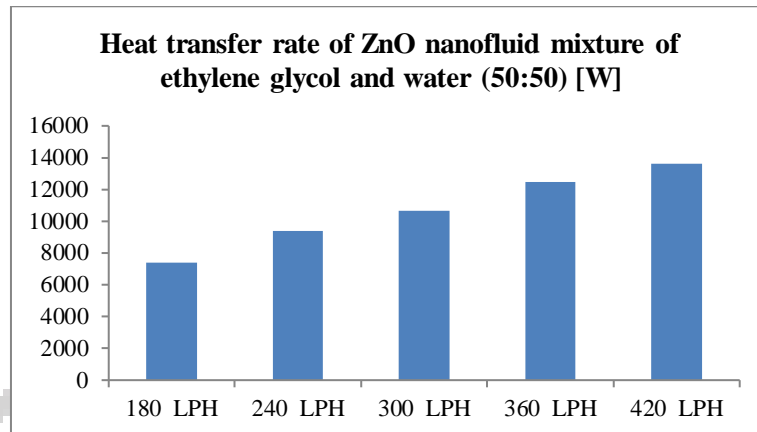


Figure 40 Outlet temperature of ZnO nanofluid mixture of ethylene glycol and water (50:50)

From the above graph it has been observed that as the flow rates of the nanofluid coolant were increased the outlet temperature increases, at 180 LPH 53.14°C, at 240 LPH 56.54°C, at 300 LPH 56.86°C, at 360 LPH 59.02°C & at 420 LPH 61.8°C. The maximum outlet temperature of 16.29 % increased at 420 LPH as compared with 180 LPH.



**Figure 41 Heat transfer rate of ZnO nanofluid mixture of ethylene glycol and water (50:50)**

From the above graph it has been observed that as the flow rates of the nanofluid coolant were increased the heat transfer rate increases, at 180 LPH 7402.59 W, at 240 LPH 9407.68 W, at 300 LPH 10648.81 W, at 360 LPH 12443.43 W & at 420 LPH 13592.17 W. The maximum heat transfer rate of 83.6 % increased at 420 LPH as compared with 180 LPH.

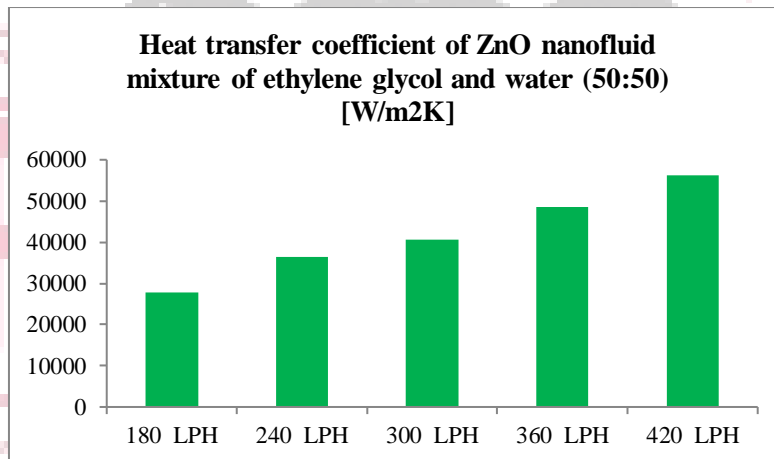


**Figure 42 Heat transfer coefficient of ZnO nanofluid mixture of ethylene glycol and water (50:50)**

From the above graph it has been observed that as the flow rates of the nanofluid coolant were increased the heat transfer coefficient increases, at 180 LPH 27908.43 W/m<sup>2</sup>K, at 240 LPH 36529 W/m<sup>2</sup>K, at 300 LPH 40647.27 W/m<sup>2</sup>K, at 360 LPH 48591.4 W/m<sup>2</sup>K & at 420 LPH 56221.75 W/m<sup>2</sup>K. The maximum heat transfer rate of 1.015 times increased at 420 LPH as compared with 180 LPH.

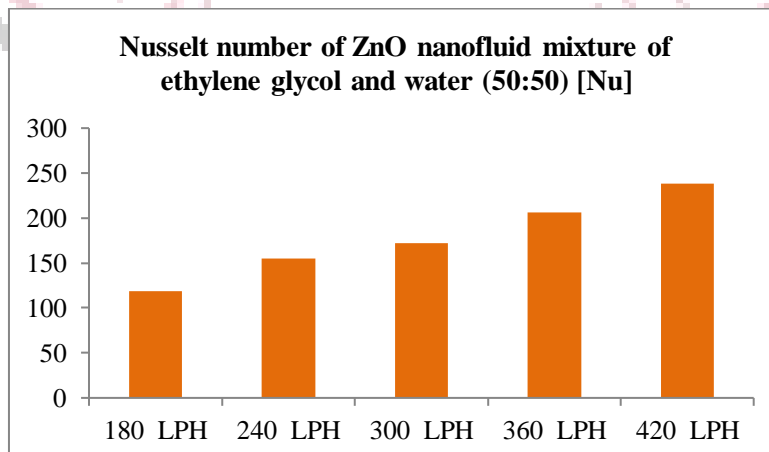


**Figure 43 Nusselt number of ZnO nanofluid mixture of ethylene glycol and water (50:50)**

**D. Computational Fluid Dynamics Analysis for Radiator using Graphene oxide Nanofluid Mixture of Ethylene Glycol and Water Ranging from 180-420 LPH**

- **Computational Fluid Dynamics Analysis for Radiator using Graphene oxide Nanofluid Mixture of Ethylene Glycol and Water (60:40) at 180 LPH**

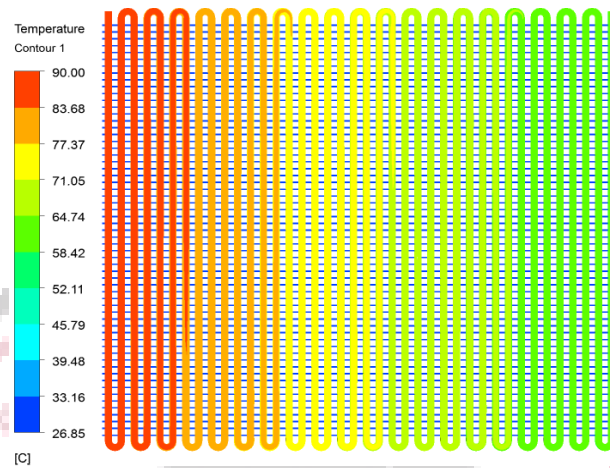


**Figure 44 Temperature distribution for graphene oxide/ethylene glycol: water (60:40)at 180LPH**

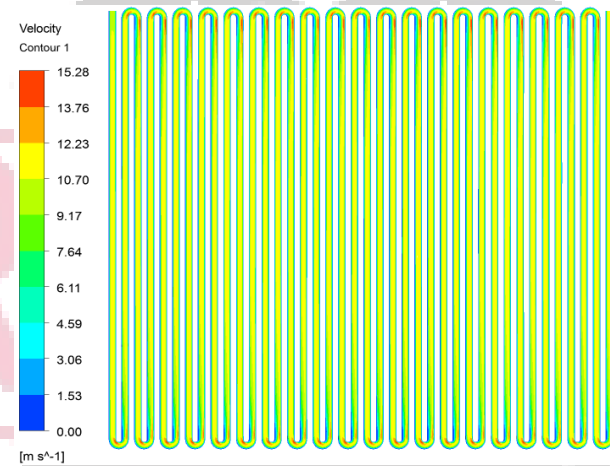


**Figure 45 Velocity distribution for graphene oxide/ethylene glycol: water (60:40)at 180LPH**

- **Computational Fluid Dynamics Analysis for Radiator using Graphene Oxide Nanofluid Mixture of Ethylene Glycol and water (60:40) at 240 LPH**

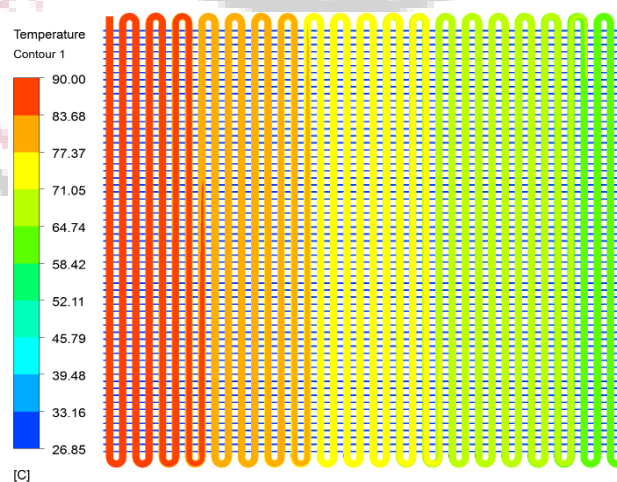


**Figure 46 Temperature distribution for graphene oxide/ethylene glycol:water (60:40)at 240LPH**

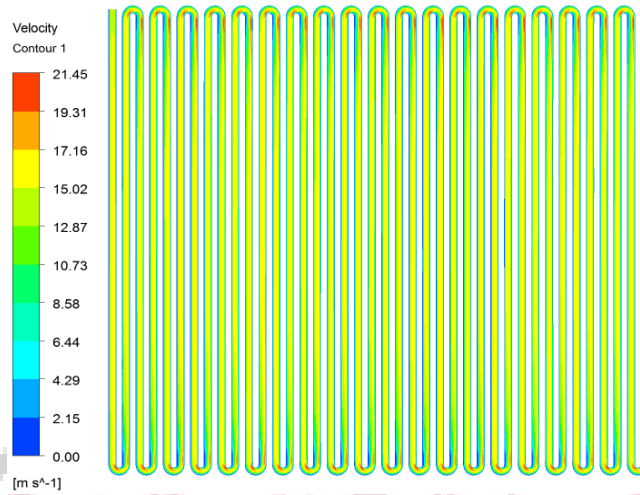


Figure 47 Velocity distribution for graphene oxide/ethylene glycol:water (60:40) at 240LPH

- **Computational Fluid Dynamics Analysis for Radiator using Graphene oxide Nanofluid Mixture of Ethylene Glycol and Water (60:40) at 300 LPH**

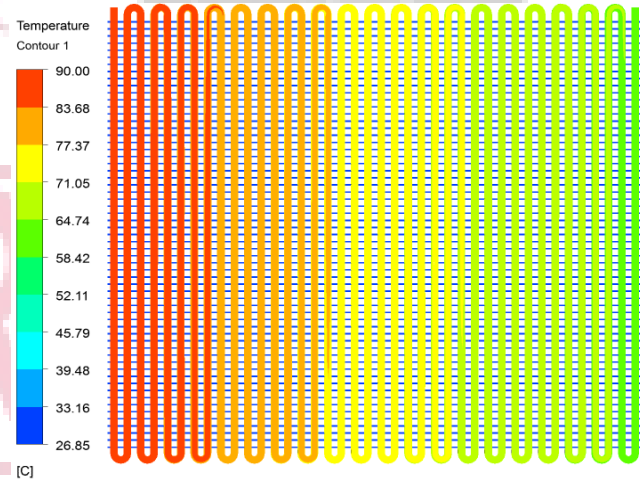


Figure 48 Temperature distribution for graphene oxide/ethylene glycol:water (60:40) at 300LPH

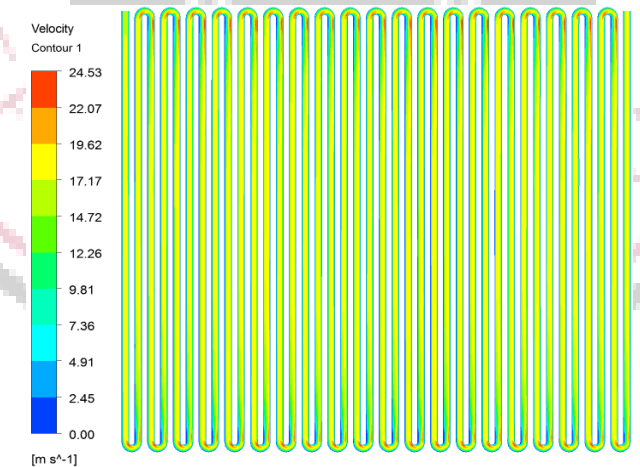
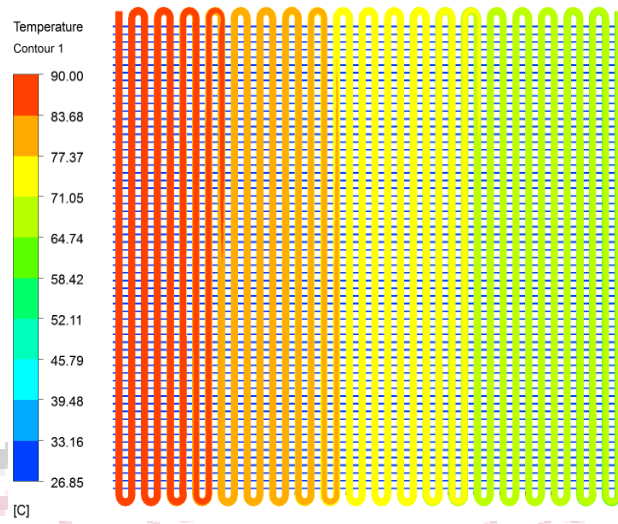
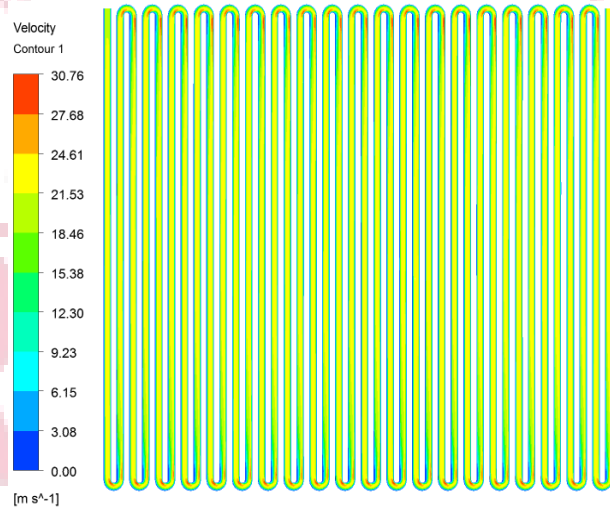


Figure 49 Velocity distribution graphene oxide/ethylene glycol: water (60:40) at 300LPH

- **Computational Fluid Dynamics Analysis for Radiator using Graphene oxide nanofluid mixture of ethylene glycol and water (60:40) at 360 LPH**



**Figure 50 Temperature distribution for graphene oxide/ethylene glycol: water (60:40)at 360LPH**



**Figure 51 Velocity distribution graphene oxide/ethylene glycol:water (60:40)at 360LPH**

- **Computational Fluid Dynamics Analysis for Radiator using Graphene Oxide Nanofluid Mixture of Ethylene Glycol and Water (60:40) at 420 LPH**

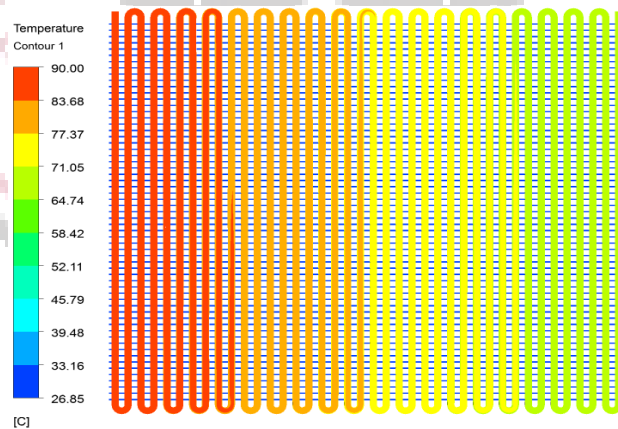


**Figure 52 Temperature distribution for graphene oxide/ethylene glycol:water (60:40)at 420LPH**

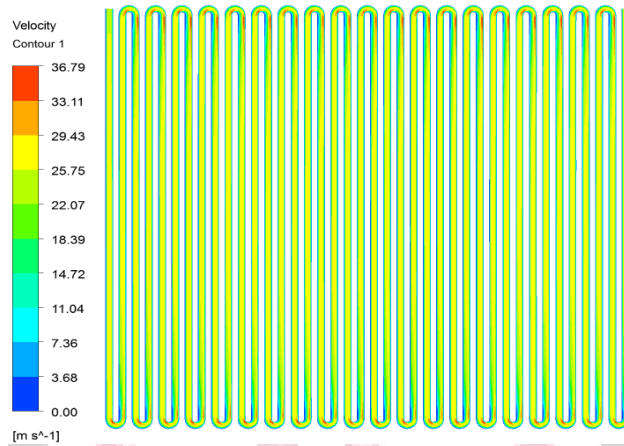


Figure 53 Velocity distribution for graphene oxide/ethylene glycol:water (60:40)at 420LPH

Table 7 Comparative results of temperature difference & heat transfer rate for graphene oxide/ethylene glycol: water (60:40)

Mass flow rate [LPH]	Inlet Temperature [°C]	Outlet temp [°C]	Temperature Difference $\Delta T$	Heat transfer rate [W]
180	90	60.23	29.77	5253.97
240	90	62.82	27.18	6715.63
300	90	62.97	27.03	7632.64
360	90	65.08	24.92	8796.04
420	90	67.21	22.79	9653.05

Table 8 Comparative results of Reynolds number, Nusselt number & heat transfer coefficient for graphene oxide/ethylene glycol: water (60:40)

Mass flow rate [LPH]	Reynolds number [Re]	Nusselt number [Nu]	Convective heat transfer coefficient [W/m <sup>2</sup> K]
180	9404.66	82.60	15143.47
240	13166.52	108.12	19821.11
300	15047.45	120.30	22055.73
360	18809.32	143.82	26366.32
420	22571.18	166.40	30506.64

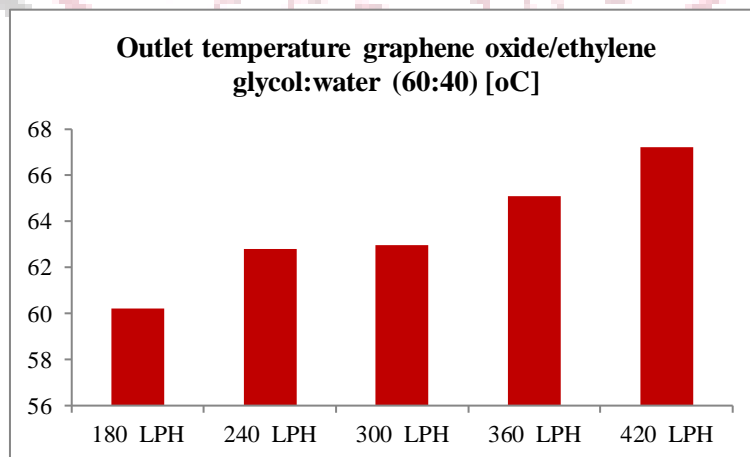
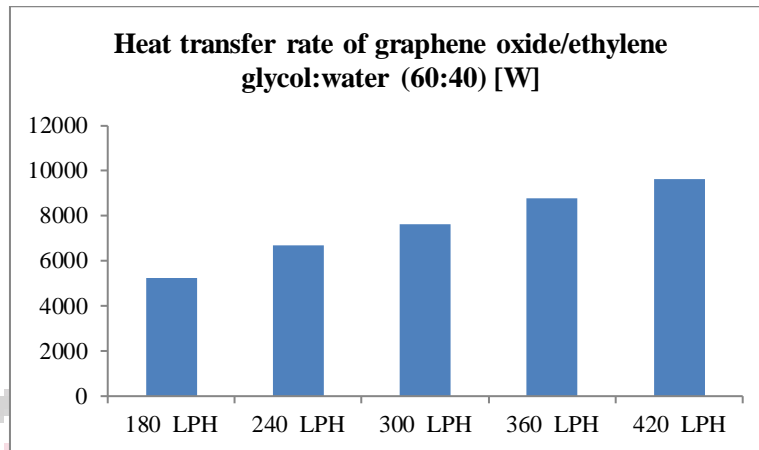


Figure 54 Outlet temperature of Grapheme oxide/ethylene Glycol: water (60:40)

From the above graph it has been observed that as the flow rates of the nanofluid coolant were increased the outlet temperature increases, at 180 LPH 60.23 °C, at 240 LPH 62.82 °C, at 300 LPH 62.97 °C, at 360 LPH 65.08 °C & at 420 LPH 67.21 °C. The maximum outlet temperature of 11.59 % increased at 420 LPH as compared with 180 LPH.



**Figure 55 Heat transfer rate of graphene oxide/ethylene glycol: water (60:40)**

From the above graph it has been observed that as the flow rates of the nanofluid coolant were increased the heat transfer rate increases, at 180 LPH 5253.97 W, at 240 LPH 6715.63 W, at 300 LPH 7632.64 W, at 360 LPH 8796.04 W & at 420 LPH 9653.05 W. The maximum heat transfer rate of 83.7 % increased at 420 LPH as compared with 180 LPH.

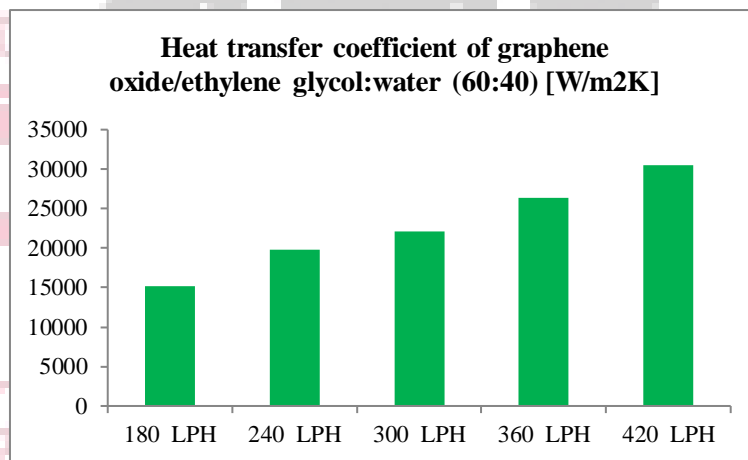


**Figure 56 Heat transfer coefficient of graphene oxide/ethylene glycol water (60:40)**

From the above graph it has been observed that as the flow rates of the nanofluids coolant were increased the heat transfer coefficient increases, at 180 LPH 15143.47 W/m<sup>2</sup>K, at 240 LPH 19821.11 W/m<sup>2</sup>K, at 300 LPH 22055.73 W/m<sup>2</sup>K, at 360 LPH 26366.32 W/m<sup>2</sup>K & at 420 LPH 30506.64 W/m<sup>2</sup>K. The maximum heat transfer rate of 1.015 times increased at 420 LPH as compared with 180 LPH.

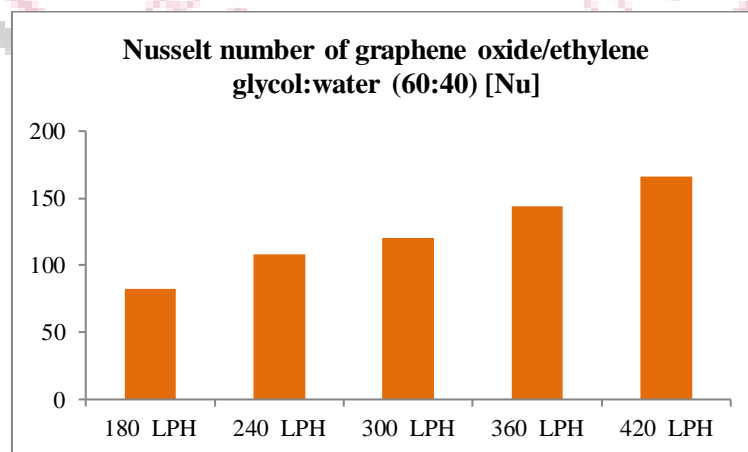


**Figure 57 Nusselt number of graphene oxide/ethylene glycol:water (60:40)**

From the above graph it has been observed that as the flow rates of the nanofluid coolant were increased the value of Nusselt number increases, at 180 LPH 82.6, at 240 LPH 108.12, at 300 LPH 120.3, at 360 LPH 143.82 & at 420 LPH 166.4. The maximum Nusselt number of 1.015 times increased at 420 LPH as compared with 180 LPH.

**E. Comparative Results for Rate of Heat Transfer at Different flow Rate**

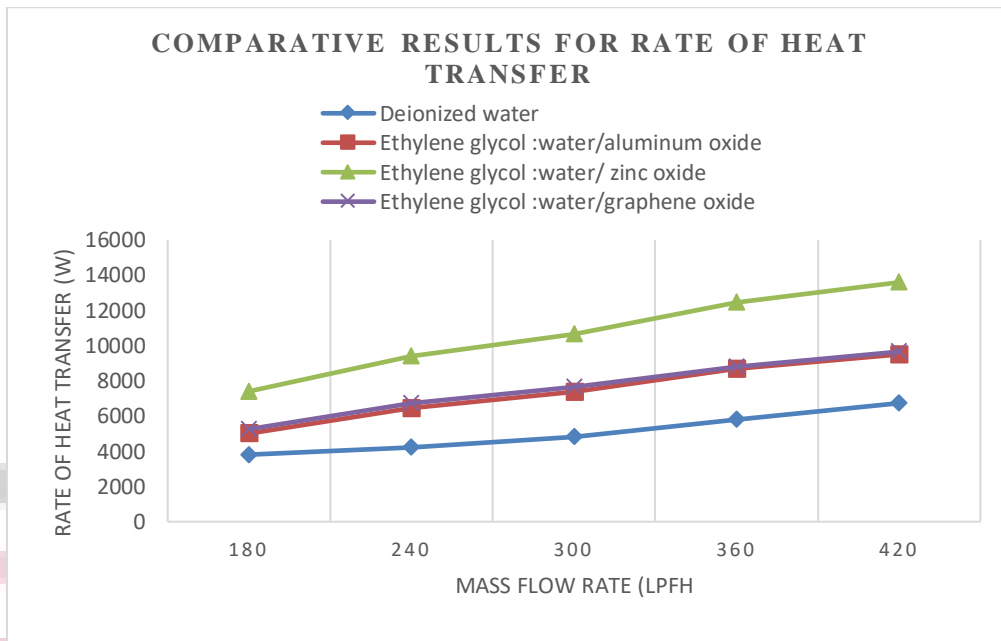


**Figure 58 Comparative results for rate of heat transfer at different flow rate**

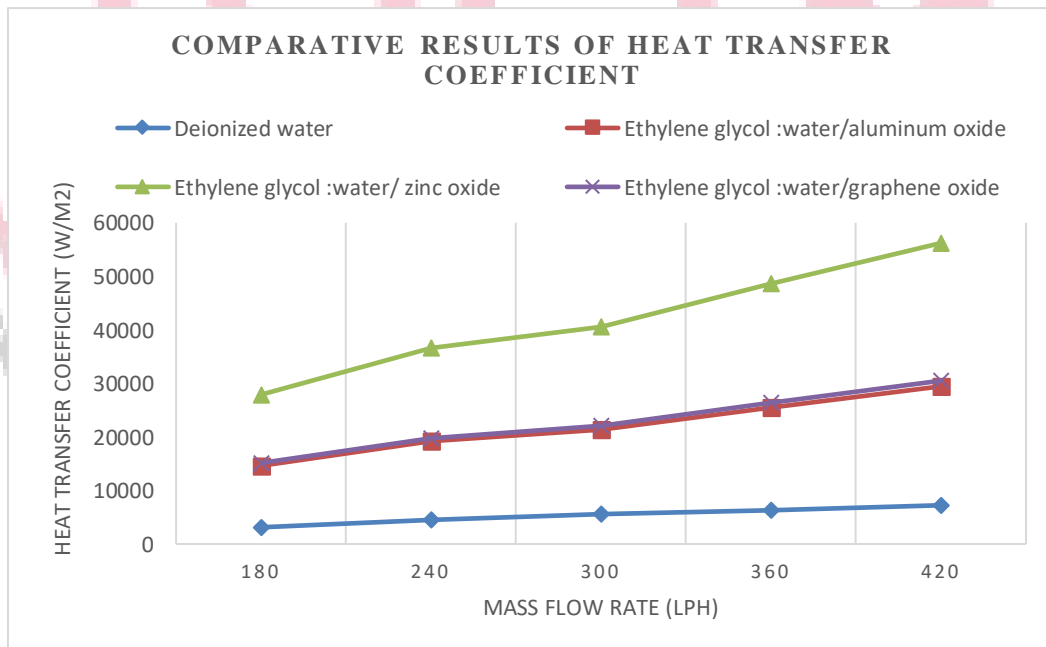


**Figure 59 Comparative results of heat transfer coefficient at different flow rate**

From the above graph of comparative results for rate of heat transfer at different flow rates, it has been observed that the maximum variation in rate of heat transfer of 77.91% for Al<sub>2</sub>O<sub>3</sub> nanofluid mixture of ethylene glycol & water (60:40), 84.34% for graphene/water-ethylene glycol (60:40) and 1.57 times enhanced for ZnO nanofluids mixture of ethylene glycol & water (50:50) at 300 LPH.



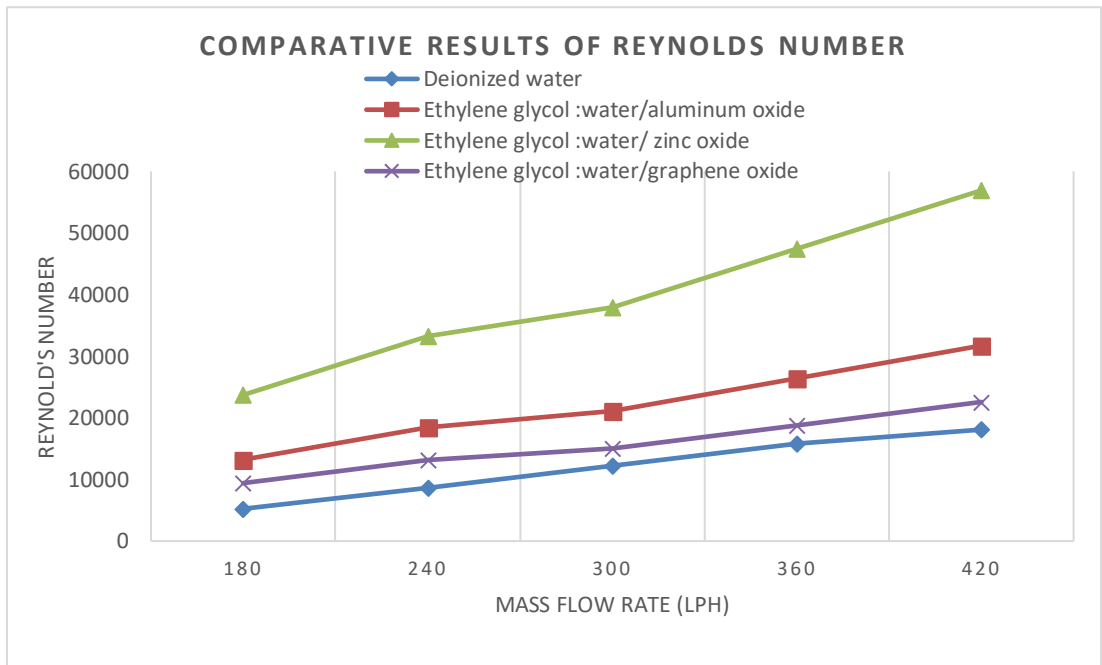


**Figure 60** Comparative results of Reynolds number at different flow rate

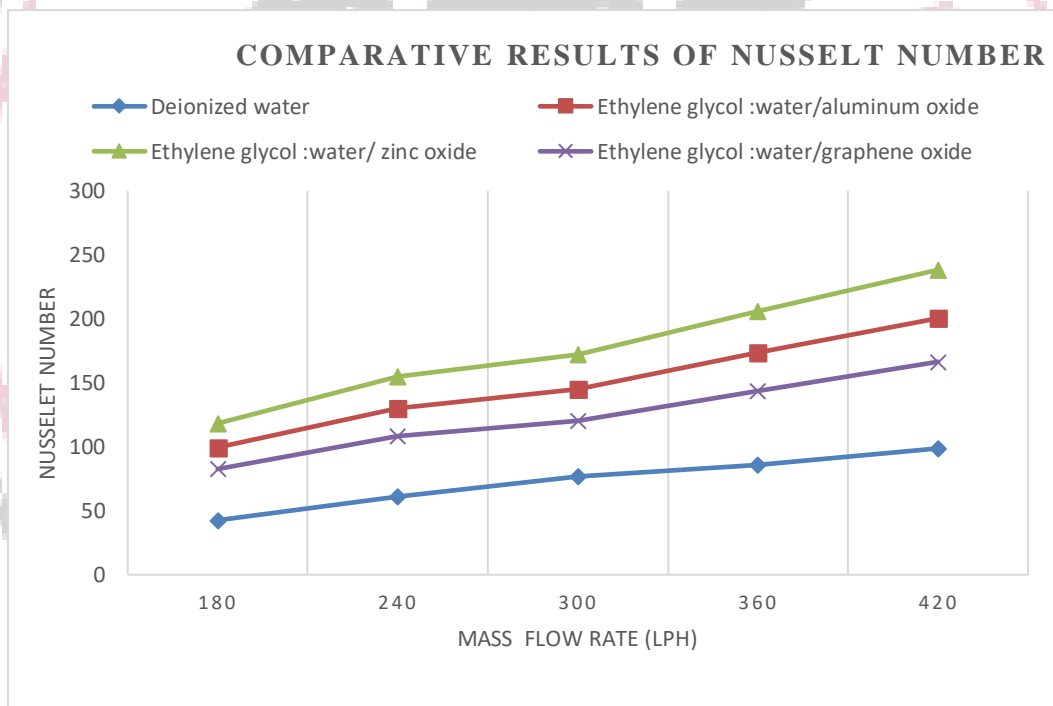


**Figure 61** Comparative results of Nusselt number at different flow rate

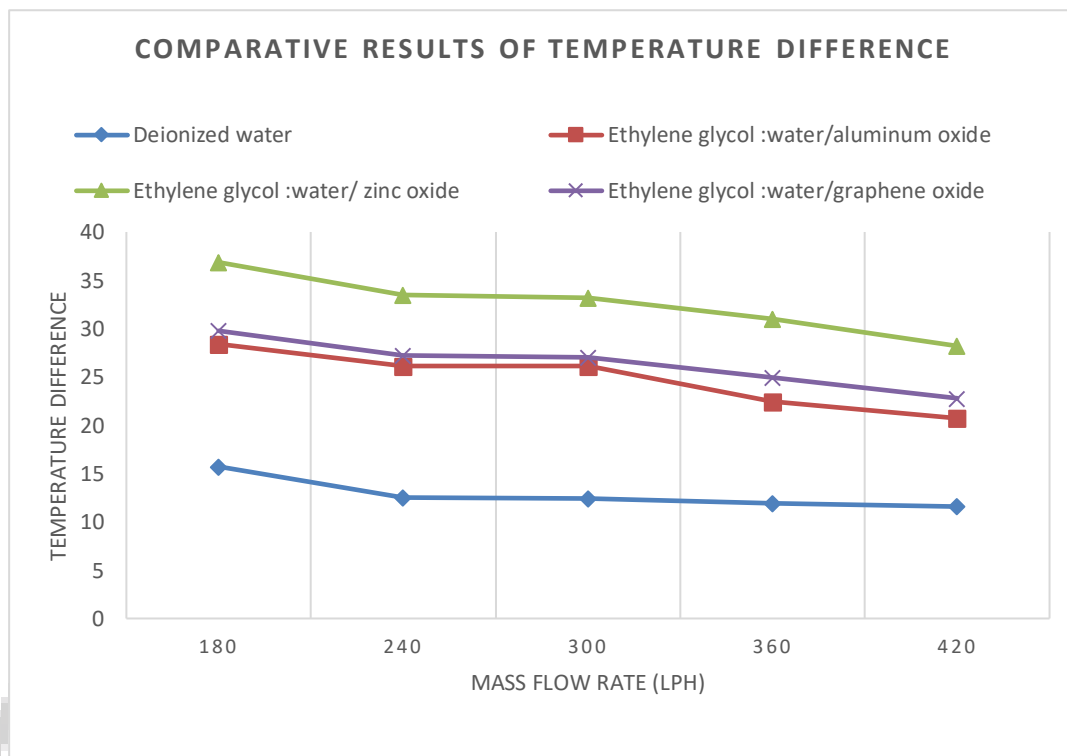


**Figure 62 Comparative results of Temperature difference at different flow rate**

From the above graph of comparative results for the temperature difference at different flow rate, it has been observed that the maximum variation of temperature difference of 1.11 times for Al<sub>2</sub>O<sub>3</sub> nanofluid mixture of ethylene glycol & water (60:40), 1.18% times for graphene Oxide nanofluid mixture of ethylene glycol & water (60:40) and 1.67 times enhanced for ZnO nanofluid mixture of ethylene glycol & water (50:50) at 300 LPH.

## V. CONCLUSION

To investigate the thermal performance of the radiator at various heat transfer fluid flow rates while using a variety of coolants, such as deionized water, a mixture of ethylene glycol and water (60:40) mixed with Al<sub>2</sub>O<sub>3</sub> nanoparticles, a combination for ethylene glycol and water (50:50) mixed with ZnO nanoparticles, and a mixture of ethylene glycol and water (60:40) mixed with graphene Oxide, mathematical and computational fluid dynamic analysis. To do this, a three-dimensional CAD radiator model was made using the design module of the ANSYS workbench, and a steady state pressure-based absolute velocity formulation assessment was defined, using the Energy equation for thermal analysis and the K-epsilon RNG viscous model with a standard wall function for turbulent flow. A heat transfer fluid mass flow intake with a range of 180 LPH to 420 LPH has been employed. The analysis discussed above led to the findings that are listed below.

## REFERENCES

- [1] Tuncay, V., & Ooijen, P. M. A. Van. (2019). 3D printing for heart valve disease: a systematic review. 0.
- [2] R. Prasanna Shankara et al. (2022) "An insight into the performance of radiator system using ethylene glycol-water based graphene oxide nanofluids" Alexandria Engineering Journal, 61, 5155–5167; <https://doi.org/10.1016/j.aej.2021.10.037>.
- [3] Pan, A.-X. et al. (2021) "Failure analysis on abnormal leakage of radiator for high-speed train transformer." Engineering Failure Analysis, 129, 105673. doi:10.1016/j.engfailanal.2021.105673.
- [4] Ijaz, H. Et al. (2020) "Effect of graphene oxide doped nano coolant on temperature drop across the tube length and effectiveness of car radiator -A CFD study." Thermal Science and Engineering Progress, 100689. doi:10.1016/j.tsep.2020.100689.
- [5] Abhilash, P. et al. (2020) "Design and testing of radiator with fixed channel and helical pipe using nanofluids." Materials Today: Proceedings, 39, 615–620. doi:10.1016/j.matpr.2020.09.002.
- [6] Kirubagharan, R. et al. (2020) "Geometrical analysis of automobile radiator using CFD." Materials Today: Proceedings. doi:10.1016/j.matpr.2020.03.739.
- [7] Nasiri, A. et al. (2019) "Intelligent fault diagnosis of cooling radiator based on deep learning analysis of infrared thermal images." Applied Thermal Engineering, 114410. doi:10.1016/j.applthermaleng.2019.114410.